RSC Advances

PAPER

View Article Online
View Journal | View Issue

Cite this: *RSC Adv.*, 2016, **6**, 85745

Synthesis, crystal structure and hydrolysis of novel isomeric cage (P–C/P–O)-phosphoranes on the basis of 4,4,5,5-tetramethyl-2-(2-oxo-1,2-diphenylethoxy)-1,3,2-dioxaphospholane and hexafluoroacetone†

Nadezhda R. Khasiyatullina,[a] Vladimir F. Mironov,*[ab] Dmitry B. Krivolapov,[a] Ekaterina V. Mironova[ab] and Oleg I. Gnezdilov[c]

Received 14th July 2016
Accepted 24th August 2016

DOI: 10.1039/c6ra17983e

www.rsc.org/advances

The reaction of 4,4,5,5-tetramethyl-2-(2-oxo-1,2-diphenylethoxy)-1,3,2-dioxaphospholane with hexafluoro acetone leads to the simultaneous formation of regioisomeric cage (P–C/P–O)-phosphoranes, the structures of which are unequivocally confirmed by XRD. The rearrangement of the P–C-isomer to P–O-isomer with high stereoselectivity (>96%) takes place in methylene chloride solution with the retention of the phosphorus coordination. It was found that the stepwise hydrolysis of the P–O-isomer initially gives 2-(2,3-dihydroxy-1,2-diphenyl-3-trifluoromethyl-4,4,4-trifluorobutyloxy)-4,4,5,5-tetramethyl-2-oxo-1,3,2-dioxaphospholane as the only stereoisomer whose structure is also confirmed by XRD. Further hydrolysis of this compound leads to the formation of 2,3-dihydroxy-3-trifluoromethyl-4,4,4-trifluoro-1,2-diphenylbutylphosphate and pinacol, which forms the solvate in the crystal. Hydrolysis of the P–C-isomer yields 2-hydroxy-4,4,5,5-tetramethyl-2-oxo-1,3,2-dioxaphospholane, benzoin and hexafluoroisopropanol.

Introduction

Pentacoordinated phosphorus compounds are key intermediates in phosphoryl group transfer reactions, which are important in the processes of cell viability[1–7] and in the origin and development of life.[8] Such phosphorus derivatives are intermediates in the nucleophilic substitution reactions at the tetrahedral phosphorus atom,[9–13] among which the most important for organic synthesis are the Wittig,[14] Appel,[15,16] and Mitsunobu[17–19] reactions, which are well described. Therefore, the synthesis, structure and chemical transformations of phosphoranes have attracted considerable attention.[20–27] Among the diverse synthetic methods for the preparation of phosphoranes, several general approaches based on the addition reactions of P(III)-derivatives to unsaturated systems, various reactions of tetracoordinated phosphorus and substitution reactions at P(V)[28,29] should be noted.

Recently, we developed a new approach for the preparation of phosphoranes based on the cascade reactions of P(III)-derivatives, containing an unsaturated moiety with carbonyl compounds, which leads to P(V)–C cage heterocycles.[30–34] Scheme 1, which shows the synthetic possibilities of this approach, is an example of the reactions of benzodioxaphosphole derivatives **1** with hexafluoroacetone. It is assumed that the reactions proceed through intermediate P^{+}–C–O^{-} bipolar ions followed by the transfer of the reactive center on the exocyclic unsaturated substituent, which lead to the formation of the corresponding cage phosphoranes **2–4** bearing the P–C-bond.[30–32]

Scheme 2 demonstrates the synthetic potential of the intramolecular cascade cyclization of P(III)-derivatives **1** under the

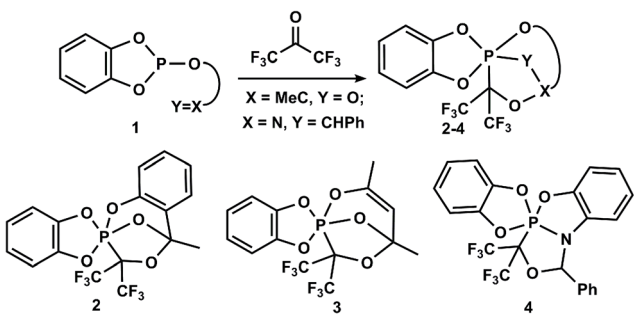

Scheme 1 Use of P(III)-derivatives bearing an exocyclic C=O or C=N bond in the synthesis of cage phosphoranes.

[a]*A. E. Arbuzov Institute of Organic and Physical Chemistry, Russian Academy of Sciences, Arbuzov Str. 8, 420088 Kazan, Russia. E-mail: mironov@iopc.ru*

[b]*Kazan (Volga Region) Federal University, Kremlyovskaya Str. 18, Kazan, 420008, Russia*

[c]*E. K. Zavoisky Kazan Physical-Technical Institute, Russian Academy of Sciences, Sibirskiy Trakt 10/7, Kazan, 420029, Russia*

† Electronic supplementary information (ESI) available: NMR and IR spectra of new compounds and crystallographic data. CCDC 1474601–1474604, 1485824. For ESI and crystallographic data in CIF or other electronic format see DOI: 10.1039/c6ra17983e

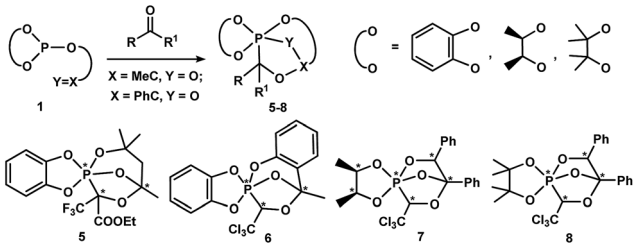

Scheme 2 Reaction of P(III)-derivatives **1** bearing an exocyclic C=O bond with trifluoropyruvic acid ethyl ester and chloral.

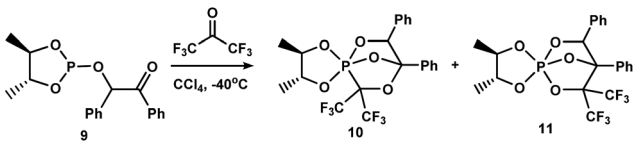

Scheme 3 Simultaneous formation of PCO- and POC-isomers **10** and **11** in the reaction of phospholane **1** with hexafluoroacetone.

action of prochiral trifluoropyruvic acid ethyl ester and chloral, which allows the P–C-cage phosphoranes **5–8** to be obtained with high stereoselectivity.[33,34]

None of these reactions afford pentaalkoxyphosphoranes, the products of intramolecular PCO/POC-rearrangement, which is characteristic to the reaction of ordinary trialkylphosphites with the carbonyl compounds mentioned above.[35,36]

Recently, we have shown[37] that the inclusion of a phosphorus(III) atom in the dioxaphospholane cycle results in the simultaneous formation of PCO- and POC-isomers (1 : 1) of cage phosphoranes[10,11] in the reaction of 4,5-dimethyl-2-(2-oxo-1,2-diphenylethoxy)-1,3,2-dioxaphospholane[9] with hexafluoro acetone (Scheme 3). PCO-phosphorane **10** is subjected to intramolecular PCO/POC-rearrangement during storage (CH_2Cl_2, 20 °C, 30 days) and yields the POC-species **11**.

Results and discussion

Considering that the related PCO/POC-rearrangement in a series of 1-hydroxyalkylphosphonates (–phosphinates) is facilitated not only by electron-withdrawing substituents at the carbon atom bonded with OH-group, but also electron-donor substituents at the phosphorus atom,[38] we introduced 4,4,5,5-tetramethyl-2-(2-oxo-1,2-diphenylethoxy)-1,3,2-dioxaphospholane **12** in the reaction with hexafluoroacetone. Tetramethyl-substituted dioxaphospholane **12** has essentially more electron donor cyclic moieties as compared with the dimethyl-substituted phospholane **9**, which, however, also effectively stabilizes the phosphorus pentacoordinated state. Compound **12** was obtained by the phosphorylation of benzoin with 2-chloro-4,4,5,5-tetramethyl-1,3,2-dioxaphospholane in the presence of triethylamine according to the data.[39]

The reaction of phosphite **12** with hexafluoroacetone proceeds in mild conditions (CCl_4, −40 °C) with the simultaneous formation of two isomeric pentacoordinated phosphorus species **13** and **14** (Scheme 4), which have two high-field signals at δ_P −24.5 and δ_P −26.5 ppm in a ratio of 10 : 1 in their ^{31}P–$\{^1H\}$ NMR spectra (a day after the reaction). The molecular ion peaks for compounds **13** and **14** are identical (ESI, *m*/*z* 523.9) and correspond to the reaction products with a composition of 1 : 1, and their fragmentation is not significantly different. After the removal of the solvent, the oily residue crystallizes with the formation of compound **13** during storage. It manifests itself as a doublet in the high-field region (CCl_4, δ_P −25.1 ppm, $^3J_{PCCH}$ = 15.6 Hz) of the ^{31}P–$\{^1H\}$ NMR spectrum. Taking into account the spectral data (see ESI†), we determined the structure of compound **13** to be 1-(2,3-butylenedioxy)-6,6-bis(trifluoromethyl)-3,4-diphenyl-1,2,5,7-phosphatrioxabicyclo[2.2.2.1^{1,4}]heptane. The ^{19}F NMR spectrum contains two signals at δ_F −68.48 (qd, $^4J_{FCCCF}$ = 10.3 Hz, $^3J_{PCCF}$ = 4.6 Hz) and δ_F −68.94 ppm (qd, $^4J_{FCCCF}$ = 10.3 Hz, $^3J_{PCCF}$ 2.3 Hz) with an equal integral intensity, which correspond to the non-equivalent fluorine atoms of CF_3-groups. In contrast to the abovementioned phosphite **9**, which is a hexafluoroacetone system, the formation of PC-phosphorane **13** is a kinetically preferred process.

The structure of phosphorane **13** was confirmed by single crystal XRD. The geometry of molecule **13** in the crystal (conglomerate) is shown in Fig. 1, and the main geometrical parameters (bond lengths and bond and torsion angles) are listed in the figure caption. The configuration of the chiral atoms is $P_R{}^1C_R{}^3C_S{}^4$. A small deviation in the phosphorus atom from the $O^3O^2O^6$ plane [by −0.114(2) Å] allows us to conclude that the phosphorus atom has a slightly distorted trigonal bipyramidal configuration with a planar 0.085(2) Å base, formed by the P^1, O^2, O^3 and C^6 atoms. The O^1 and O^7 atoms located in the apical positions deviate from this plane by −1.696 (5) and 1.619(5) Å, respectively [bond angle of $\hat{I}^1$–P^1–O^7 is equal to 172.4

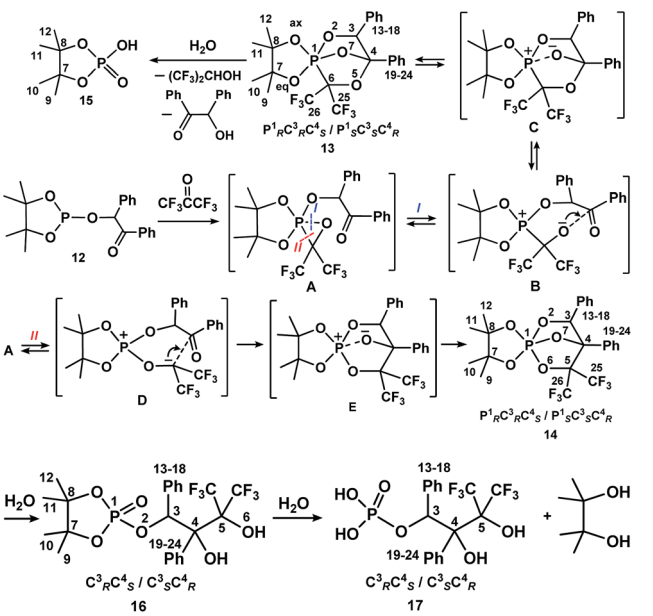

Scheme 4 The reaction of phospholane **12** with hexafluoroacetone. The same numbering of the atoms in structures **13–17** is given for convenience.

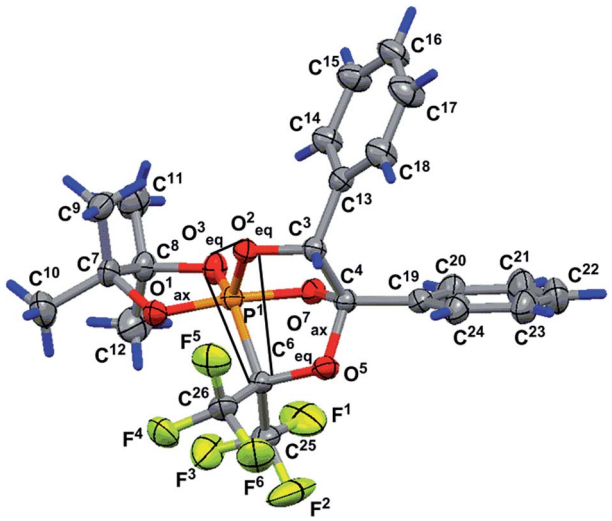

Fig. 1 Geometry of molecule **13** in a crystal (conglomerate). Selected bond lengths (Å), and bond and torsion angles (°): P^1–O^1 1.613(5), P^1–O^2 1.619(5), P^1–O^3 1.583(5), P^1–O^7 1.711(5), P^1–C^6 1.930(7), O^1–P^1–O^2 96.3(3), O^1–P^1–O^3 92.7(3), O^1–P^1–O^7 172.4(3), O^1–P^1–C^6 92.8(3), O^2–P^1–O^3 120.9(3), O^2–P^1–O^7 90.3(2), O^2–P^1–C^6 100.7(3), O^3–P^1–O^7 85.7(2), O^3–P^1–C^6 136.9(3), O^7–P^1–C^6 83.3(3), C^9–C^7–C^8–C^{12} −161.4(8), P^1–O^7–C^4–C^{19} 177.5(5), C^{13}–C^3–C^4–C^{19} 46.2(8) and O^7–C^4–C^{19}–C^{20} 1(1). Hereinafter, non-hydrogen atoms are shown in view of thermal ellipsoids with a probability of 30%, and the trigonal pyramid base is outlined with thin lines.

(3°)]. One of the two trifluoromethyl groups ($C^{25}F_3$) is almost in this plane [C^{25} atom deviation from it is 0.21(1) Å]. The O^1–P^1–O^3, O^1–P^1–O^2, O^1–P^1–C^6, O^2–P^1–O^7, O^7–P^1–C^6 and O^3–P^1–O^7 bond angles vary within the limits of 83.3(3)–96.9(3)°. The O^2–P^1–C^6, O^2–P^1–O^3 and O^3–P^1–C^6 bond angle sum in the pyramid base is equal to 358.5(2)° and points to a trigonal bipyramidal phosphorus configuration close to an almost regular configuration. The P^1–O^3 equatorial bond length is slightly smaller [1.583(5) Å] than the P^1–O^1 and P^1–O^7 axial bond lengths of [1.613(3) and 1.711(5) Å].

The concurrence of the P^1–O^1 and P^1–O^7 axial bond length sum [3.324(5) Å] and $O^1\cdots O^7$ distance [3.317(7) Å] can be considered as evidence of the regular trigonal bipyramidal phosphorus configuration. The P^1–C^6 bond length is equal to 1.930(7) Å. A five-membered dioxaphospholane cycle occupies the axial-equatorial position in the trigonal bipyramid (O^1 is axial and O^3 is equatorial), its conformation is *envelope*, where four atoms, O^1, P^1, O^3 and C^8, lie in one plane [planar within 0.004(5) Å], and the C^7 atom deviates from this plane by 0.518(9) Å. The C^9 and C^{12} atoms deviate from this plane by 2.05(1) and −1.43(1) Å, respectively, and they occupy axial positions in the cycle. The C^{10} and C^{11} atoms also deviate from the $O^1P^1O^3C^8$ plane by −0.05(1) and 0.91(1) Å, respectively, and are located in equatorial positions. The O^2 and C^6 atoms deviate in opposite sides from the $O^1P^1O^3C^7$ plane [their deviations are 1.377(5) and −1.297(8) Å, respectively] and occupy equatorial and axial positions in the five-membered cycle. The C^{10} and O^7 deviations are minimal [they deviate by −0.05(1) and −0.213(5) Å, respectively] and we can assume that they lie in the $O^1P^1O^3C^8$ plane.

The $O^1P^1O^3C^8$ fragment can also be considered as a part of the most elongated seven-membered approximately planar $C^8O^3P^1O^1O^7C^4C^{19}$ system [planar within 0.135(5) Å]. The plane of the phenyl substituent in the fourth position of the bicycloheptane **13** is slightly turned in the dihedral angle of 6.2(5)° relative to the seven-membered fragment. The conformation of the five-membered $P^1O^2C^3C^4O^7$ cycle of molecule **13** is *envelope* (Fig. 1). It includes a four-membered plane $P^1O^2C^3C^4$ fragment [planar within 0.025(5) Å], and the O^7 atom deviates from this plane by 0.760(5) Å. The O^1, O^3, O^5, C^6, C^{13} and C^{19} atoms deviate from the abovementioned fragment by the values of −0.742(5), 1.302(5), −1.391(5), −1.574(7), 1.257(7) and 0.355(3) Å, respectively. This is due to fact that the C^{13} and C^{19} atoms deviate to one side point out of the *cis*-orientation of the phenyl substituents in the five-membered cycle discussed above. The conformation of the other five-membered $P^1C^6O^5C^4O^7$ ring of the rigid bicycloheptane scaffold is a slightly distorted *envelope*. The four-membered $P^1C^6O^5C^4$ fragment is planar within 0.066(5) Å, and the O^7 atom deviates from this plane by −0.853(5) Å. The O^1, O^2, O^3, C^3, C^{19}, C^{25} and C^{26} atoms deviate from the abovementioned fragment by the values of −0.699(5), 1.392(5), −0.949(5), 1.337(7), −0.579(7), −1.40(1) and 1.097(9) Å, respectively.

During storage in very polar dichloromethane at 20 °C for about five days, compound **13** underwent a gradual conversion to compound **14** (after four days, the ratio of compounds **13**/**14** was 1 to 20). Fig. 2 shows the spectral image of this process according to ^{31}P–{^1H} NMR. The figure shows that phosphorane **13** (CH_2Cl_2, δ_P −25.0 ppm) was completely converted to pentaoxyphosphorane **14** (CH_2Cl_2, δ_P −26.7 ppm), which is a minor compound in the reaction in tetrachloromethane. This compound was isolated in the individual state by crystallization under a layer of pentane and characterized by spectral methods, which allowed the assignment of the structure of 1-(2,3-butylenedioxy)-5,5-bis(trifluoromethyl)-3,4-diphenyl-1,2,6,7-phosphatrioxabicyclo[2.2.$1^{1,4}$]heptane **14**, the product of PCO/POC-rearrangement. In the ^{13}C–{^1H} NMR spectrum of compound **14**, the carbon atom bonded to CF_3-groups resonates at 83.41 ppm as a septet with coupling through two bonds from fluorine ($^2J_{CCF}$ = 29.3 Hz), unlike the spectrum of compound **13** in which the oxygenated carbon in the $OC(CF_3)_2$ fragment manifests itself as a doublet of septets at 77.78 ppm with direct spin–spin coupling from phosphorus ($^1J_{PC}$ = 154.8 Hz, $^2J_{FCC}$ = 30.7 Hz). The signals of the CF_3-groups in the ^{19}F NMR spectrum of compound **14** appear as two quartets at δ_F −68.22 ppm and −72.35 ppm ($^4J_{FCCCF}$ = 9.5 Hz).

Its structure was also confirmed by single crystal XRD. Fig. 3 presents the geometry of the molecule in a crystal (the main geometrical parameters, including bond length, valence and torsion angles of the molecule above, are presented in the ESI file†). The configuration of the chiral atoms is $P_R{}^1C_R{}^3C_S{}^4/P_S{}^1$-$C_S{}^3C_R{}^4$ (racemate). The meaningless deviation of the phosphorus atom from the $O^3O^2C^6$ plane by −0.0580(7) Å allows to conclude that the geometry of phosphorus in molecule **14** is a slightly distorted trigonal bipyramid with a planar base [within 0.043(2) Å], where the P^1, O^2, O^3, C^6 atoms are located. The O^1 and O^7 atoms located in apical positions deviate from

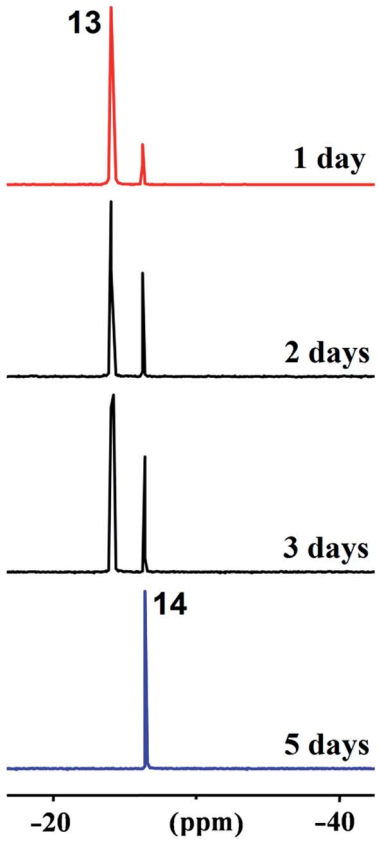

Fig. 2 Conversion of P–C-phosphorane **13** to P–O-species **14** according to $^{31}P-\{^{1}H\}$ NMR spectra (CH_2Cl_2, in one day, and after two, three and five days).

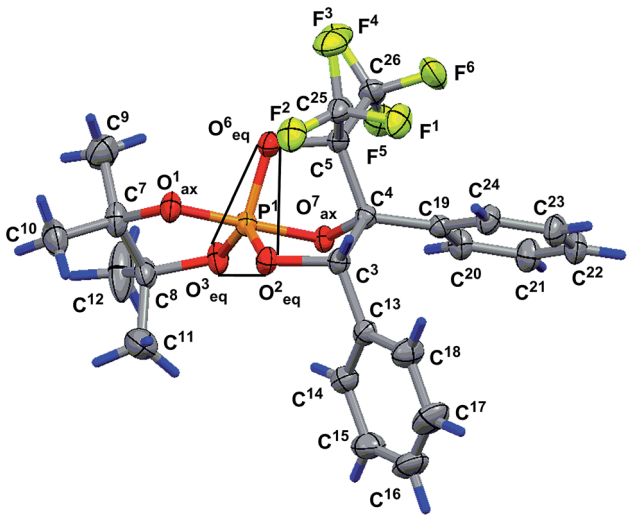

Fig. 3 Geometry of molecule **14** in a crystal (racemate, $P_S^1C_S^3C_R^4$-enantiomer is shown). The base of the trigonal bipyramid is shown by thin lines. Selected bond lengths (Å) and bond and torsion angles (°): P^1-O^1 1.625(2), P^1-O^2 1.606(2), P^1-O^3 1.582(2), P^1-O^6 1.647(2), P^1-O^7 1.700(2), $O^1-P^1-O^2$ 92.1(1), $O^1-P^1-O^3$ 92.4(1), $O^1-P^1-O^7$ 177.5(1), $O^1-P^1-O^6$ 91.6(1), $O^2-P^1-O^3$ 126.4(1), $O^2-P^1-O^7$ 90.4(1), $O^2-P^1-O^6$ 105.8(1), $O^3-P^1-O^7$ 86.1(1), $O^3-P^1-O^6$ 127.4(1), $O^6-P^1-O^7$ 87.8(1), $C^9-C^7-C^8-C^{11}$ −164.4(4), $P^1-O^7-C^4-C^{19}$ 178.8(2), $C^{13}-C^3-C^4-C^{19}$ −40.9(3) and $O^7-C^4-C^{19}-C^{20}$ 10.0(4).

the above plane by the values of −1.625(2) and 1.700(2) Å [the valence angle of $O^1-P^1-O^7$ is equal to 177.5(1)°]. The values of the valence angles $O^1-P^1-O^3$, $O^1-P^1-O^2$, $O^1-P^1-O^6$, $O^2-P^1-O^7$, $O^6-P^1-O^7$ and $O^3-P^1-O^7$ vary within the limits of 86.1(1)–92.4(1)°, and the sum of the valence angles of $O^2-P^1-O^6$, $O^2-P^1-O^3$ and $O^3-P^1-O^6$ at the pyramid base is 359.6(2)°, which also indicate the trigonal-bipyramidal configuration of the phosphorus atom close to the regular configuration. The equatorial P^1-O^2, P^1-O^3 and P^1-O^6 bonds [1.606(2), 1.582(2), and 1.647(2) Å, respectively] are slightly shorter than the axial P^1-O^1 and P^1-O^7 bonds [1.625(2) and 1.700(2) Å, respectively]. The fact of practical coincidence of the P^1-O^1 and P^1-O^7 axial bond values sum [3.325(5) Å] and $O^1\cdots O^7$ distance [3.323(7) Å] is in favor of the regular trigonal bipyramid configuration. The five-membered tetramethyldioxaphospholane cycle occupies the axial-equatorial position in the trigonal bipyramid (O^1 atom is axial and O^3 atom is equatorial). Its conformation is a distorted *envelope*, where four O^1, P^1, O^3 and C^7 atoms lie in one plane [planar within 0.0482(7) Å], and the C^8 atom deviates from the above plane by 0.422(4) Å. The C^9 and C^{12} atoms deviate from the plane to the opposite sides by the rather significant distances of −1.525(5) and 1.963(6) Å, respectively (they occupy axial positions in the cycle), and the C^{10} and C^{11} atoms also deviate by the different values of 0.758(5) and −0.178(6) Å (they occupy equatorial positions in the cycle). The O^2 and O^6 atoms deviate to opposite sides from the $O^1P^1O^3C^7$ plane and occupy equatorial and axial positions in the five-membered cycle [their deviations are 1.182(2) and −1.406(2) Å, respectively]. The O^7 atom deviation is minimal [−0.213(5) Å]; thus, it can be concluded that this atom lies in the $O^1P^1O^3C^7$ plane. Moreover, it should be noticed that the $O^1P^1O^3C^7$ fragment is turned to be a part of the more extended planar moiety of $C^7O^3P^1O^1O^3O^7C^4C^{19}$ in the molecule [planar within 0.054(4) Å]. The plane of the phenyl substituent position 4 (C^{19-24}) is slightly turned to this seven-membered fragment [the dihedral angle between the corresponding planes is larger than the angle in molecule **13** and is equal to 9.2(2)°]. The conformation of the five-membered $P^1O^2C^3C^4O^7$ cycle of the rigid bicycloheptane system of molecule **14** is an *envelope* [it contains a planar four-membered $P^1O^2C^3C^4$ fragment within 0.033(2) Å, and the O^7 atom deviates from it by 0.806(2) Å]. The $\hat{I}^1$, O^3, C^5, O^6, C^{13} and C^{19} atoms deviate from the abovementioned planar fragment by values of −0.726(2), 1.224(2), −1.428(3), −1.341(2), 1.276(3) and 0.485(3) Å, respectively. The fact that the C^{13} and C^{19} atoms deviate to one side suggests the *cis*-orientation of the phenyl substituents in the abovementioned five-membered cycle. The conformation of the other five-membered $P^1O^6C^5C^4O^7$ cycle of the rigid bicycloheptane system of molecule **14** is a slightly distorted *envelope* [four-membered $P^1O^6C^5C^4$ fragment is planar within 0.044(3) Å, and the O^7 atom deviates from the above fragment by −0.851(2) Å]. The O^1, O^2, O^3, C^3, C^{19}, C^{25} and C^{26} atoms deviate from the abovementioned planar fragment by the values of 0.804(2), 1.364(2), −1.078(2), 1.322(3), −0.576(3), 1.366(4) and −1.151(4) Å.

Considering that compounds **13** and **14** are formed simultaneously under very mild conditions (−40 °C) and the rearrangement of P–C-isomer **13** into P–O-isomer **14** is slow, it can

be assumed that they are formed from the common unstable phosphorane intermediate **A**, which contains an oxaphosphirane cycle (Scheme 4). This intermediate is a product of the symmetry allowed [1 + 2]-cycloaddition reaction of phosphorus to the double bond of hexafluoroacetone. At low temperature, the cleavage of the three-membered ring occurs readily in two directions, ***I*** and ***II***, which finally results in the formation of compounds **13** and **14**. The direction ***I***, which includes P–O bond cleavage and the formation of intermediate bipolar ions **B** and **C**, is a kinetically controlled and reversible process. Direction ***II***, which includes P–C bond cleavage and the formation of intermediate bipolar ions **D** and **E**, irreversibly results in a thermodynamically controlled reaction product, the P–O-isomer **14**. Thus, the driving force of the PCO/POC-rearrangements seems to be the greater thermodynamic stability of the resulting pentaalkoxyphosphorane **14** in comparison with its P–C-analogue **13**. Furthermore, oxygen is more electronegative than carbon, and it is important for the stabilization of the phosphorus trigonal bipyramid, which increases its stability when acceptors are introduced to the phosphorus atom.

Due to the fact that racemic benzoin was used in the synthesis of phospholane **12** and in the reaction with hexafluoroacetone another chiral carbon (C^4) formation occurred, two P–C diastereoisomers of isomer **13** should be formed. The formation of only one diastereoisomer indicates the high stereoselectivity of the second chiral center (C^4) formed, which is probably due to the rigid spatial requirements for the attack of the alkoxide-anion to the carbonyl group of the bipolar ion **B**. The very important fact that the relative configuration of the chiral C^3 and C^4 atoms in the P–C- and P–O-isomers **13** and **14**, according to XRD data, is the same indicates the highly stereoselective nature of the intramolecular PCO/POC-rearrangement.

Hydrolysis of P–C-isomer **13** leads to the formation of dioxaphospholane **15**, benzoin, and hexafluoroisopropanol. Benzoin and compound **15** were isolated by crystallization of the reaction mixture from diethyl ester. The structures of benzoin and hexafluoroisopropanol were proven by comparison of their spectral characteristics (^{1}H, ^{13}C and ^{19}F NMR) with the literature.[40–43] The structure of dioxaphospholane **15** was established based on the comparison of its spectral parameters with that described in the literature[44,45] and XRD.

The geometry of the molecule in a crystal (solvate with one water molecule) is presented in Fig. 4. The five-membered cycle of molecule **15** has an *envelope* conformation, accordingly with a planar $O^1P^1O^3C^8$ fragment within 0.115(4) Å, and the C^7 atom deviates from the abovementioned plane by −0.492(8) Å. The O^2, C^9 and C^{12} atoms are located in axial positions (they deviate from the $O^1P^1O^3C^8$ plane by 1.574(5), −1.990(8) and 1.552(8) Å, respectively). The O^4, C^{10} and C^{11} atoms are located in equatorial positions and deviate from the $O^1P^1O^3C^8$ plane by −0.851(4), 0.20(1) and −0.713(9) Å, respectively. Due to the presence of solvent water molecules in the crystal of **15**, a classical hydrogen bond system is realized with the participation of the phosphoryl O^4 oxygen and water molecule protons [O^{1S}–$H^{1S}\cdots O^4$-interaction, the parameters are O^{1S}–H^{1S} 0.72(9) Å, $H^{1S}\cdots O^4$ 2.0(1) Å, $O^{1S}\cdots O^4$ 2.75(1) Å, $\angle O^{1S}$–$H^{1S}\cdots O^4$ 178(8)°, and symmetry operation $-1/2 + x$, $1/2 - y$, $1 - z$] and also between hydrogen at the O^2 atom and water oxygen O^{1S} [O^2–$H^2\cdots O^{1S}$-interaction, the parameters are O^2–H^2 0.86(7) Å, $H^2\cdots O^{1S}$ 1.61(7) Å, $O^2\cdots O^{1S}$ 2.46(1) Å, $\angle O^2$–$H^2\cdots O^{1S}$ 168(9)°, and symmetry operation $1 + x$, y, z]. Using the classical hydrogen interactions, the molecules in the crystal **15** form ribbons along the 0a crystallographic axis (see Fig. 5).

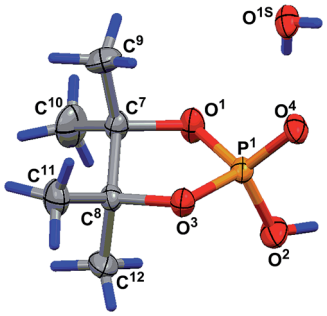

Fig. 4 Geometry of molecule **15** in a crystal (solvate with water). Selected bond lengths (Å) and bond and torsion angles (°): P^1–O^1 1.568(6), P^1–O^2 1.533(7), P^1–O^3 1.572(6), P^1–O^4 1.477(6), O^1–P^1–O^3 98.6(2), O^1–P^1–O^2 108.5(3), O^2–P^1–O^4 113.5(3), O^1–C^7–C^8–O^3 36.9(6), C^9–C^7–C^8–C^{11} 33.6(8) and C^{10}–C^7–C^8–C^{12} 34.5(8).

Mild stepwise hydrolysis of P–O-isomer **14** leads to the initial formation of dioxaphospholane **16**. The ^{31}P NMR spectrum of this compound contains a doublet (δ_P 11.0 ppm, $^3J_{PCCH}$ 5.9 Hz) with a coupling constant from the proton at C^3, which indicates the retention of the P–O–C^3 fragment. Its ^{13}C NMR spectrum shows spin–spin coupling of all the methyl carbons with the phosphorus atom, which clearly points to the retention of the 4,4,5,5-tetramethyl-1,3,2-dioxaphospholane cycle. This data are in accordance with the breaking of the P^1–O^2 and P^1–O^7 bonds in phosphorane **14** during hydrolysis. The result of the hydrolysis of phosphorane **14** differs by one for compound **11**, which

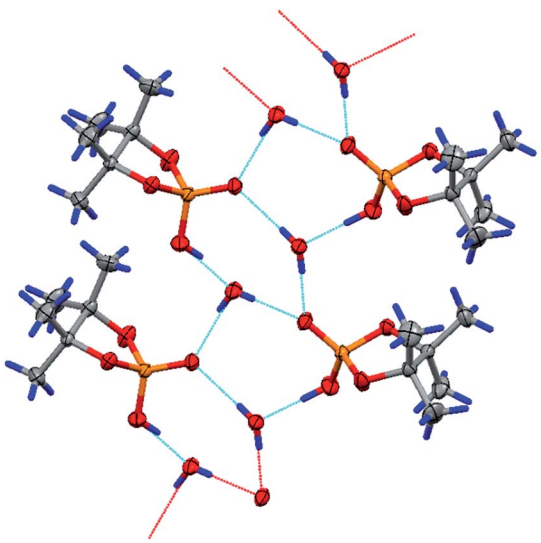

Fig. 5 System of the intermolecular hydrogen bonds in a crystal of compound **15**.

contains a 4,5-dimethyl-1,3,2-dioxaphospholane moiety. In the last case, the 2,3-butanediol elimination proceeds.[37]

The structure of phospholane **16** was confirmed using single crystal XRD. In Fig. 6, the geometry of the molecule in a crystal is presented (the main geometrical parameters, including bond length and valence and torsion angles of molecule **16** are presented in the ESI†). The phosphorus atom has a distorted tetrahedral configuration. The dioxaphospholane cycle has an *envelope* conformation with a planar four-membered $O^1P^1O^3C^7$ fragment within 0.080(6) Å, and the C^8 atom deviates from this plane by 0.510(9) Å (see Fig. 7). The O^2, C^{10} and C^{12} atoms are in axial positions (they deviate from the $O^1P^1O^3C^8$ plane by the values of 1.260(5), −1.52(1) and 2.05(1) Å, respectively). The O^4, C^9 and C^{11} atoms are in equatorial positions (they deviate from the $O^1P^1O^3C^8$ plane by the values of −1.265(6), 0.74(1) and −0.05(1) Å, respectively). The presence of four methyl groups leads to a noticeable deviation of conformation along the C^7–C^8 bond from the regular staggered *gauche* conformation due to steric repulsion (the torsion angles $C^9C^7C^8C^{12}$ and $C^{10}C^7C^8C^{11}$ are equal to −39(1) and −36(1)°, respectively). The *envelope* conformation is probably realized in a solution for the investigated compound also, which is confirmed by the non-equivalence of these four methyl groups in NMR ^{1}H and ^{13}C spectra, and also by the different spin–spin coupling constants $^3J_{PCCC}$, which depend on the P–C–C–C torsion angle values. The same situation is realized for the conformation along the C^3–C^4 bond (the torsion angles of $O^2C^3C^4O^7$ and $C^{13}C^3C^4C^{16}$ are 46.2(9) and −45.2(9)°, respectively). The repulsion between the two phenyl groups probably has less meaning in comparison with the phenyl and hexafluoroisopropylhydroxy substituent repulsion, which leads to the same conformation along the C^3–C^4 bond (the torsion angle of $C^5C^4C^3C^{13}$ is −166.7(7)°). Due to the classical hydrogen bond, O^6–$H^6\cdots O^4$, the molecules of **16** are connected in dimers, and thus, a 0D supramolecular structure is realized in the crystal [the parameters of the interaction are O^6–H^6 0.66(6) Å, $H^6\cdots O^4$ 2.14(6) Å, $O^6\cdots O^4$ 2.76(1) Å, $\angle O^6$–$H^6\cdots O^4$ 155(7)°, and symmetry operation $1-x$, $2-y$, $-z$]. The packing of the molecules in the crystal of **16** is also stabilized by the intramolecular bifurcate O^7–$H^7\cdots F^1$ and O^7–$H^7\cdots O^2$ classical hydrogen bonds [the parameters are O^7–H^7 0.87(8) Å, $H^7\cdots F^1$ 2.34(9) Å, $O^7\cdots F^1$ 2.860(9) Å, $\angle O^7$–$H^7\cdots F^1$ 119(8)°; and $H^7\cdots O^2$ 2.20(7) Å, $O^7\cdots O^2$ 2.722(8) Å, $\angle O^7$–$H^7\cdots O^2$ 118(6)° respectively, see Fig. 8].

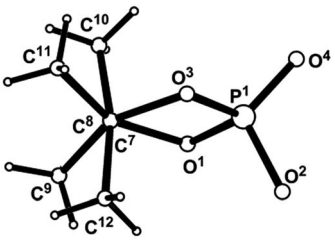

Fig. 7 Conformation of 1,3,2-dioxaphospholane cycle along the C^7–C^8 bond in **16** (acyclic substituent is omitted for clarity).

Prolonged hydrolysis of phosphorane **14** leads to the cleavage of not only the exocyclic P^1–O^6 and P^1–O^7 bonds but also the 1,3,2-dioxaphospholane P–O bonds. This process is accompanied by the formation of 2,3-dihydroxy-3-trifluoromethyl-4,4,4-trifluoro-1,2-diphenylbutylphosphate **17** and pinacol. It should be noted that phosphate **17** (δ_P −1.4 ppm, δ_F −67.05 and −67.82 ppm ($CDCl_3$/DMSO-d_6, 3 : 1)) exists in equilibrium with the cyclic form **19** (δ_P 14.7 ppm (CD_3CN), δ_F −68.42 and −69.98 ppm ($CDCl_3$/DMSO-d_6, 3 : 1)) (Scheme 5) in a solution.[37] The ratio of cyclic and acyclic phosphates in the reaction medium is close to 1 : 10; however, this equilibrium shifts to the formation of the cyclic derivative **19** upon heating (40 °C) and the ratio becomes 2 : 1. Long crystallization of the hydrolysis products from CH_2Cl_2 allowed the isolation of the crystalline complex **18** of the acyclic monophosphate **17** with pinacol in a 2 : 1 ratio. The structure of complex **18** was

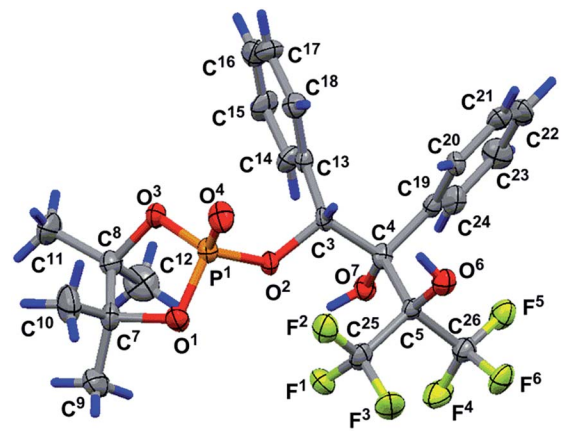

Fig. 6 Geometry of molecule **16** in a crystal (racemate, $C_R{}^3C_S{}^4$-enantiomer is shown). Selected bond lengths (Å) and bond and torsion angles (°): P^1–O^1 1.582(6), P^1–O^2 1.581(6), P^1–O^3 1.583(7), P^1–O^4 1.460(6), O^2–C^3 1.478(9), O^1–P^1–O^2 101.2(3), O^1–P^1–O^3 99.6(3), O^1–P^1–O^4 118.9(4), O^2–P^1–O^3 109.6(3), O^2–P^1–O^4 112.7(3), O^3–P^1–O^4 113.4(4), P^1–O^2–C^3–C^4 163.2(5), O^7–C^4–C^5–O^6 165.2(6) and O^2–C^3–C^4–O^7 46.1(8).

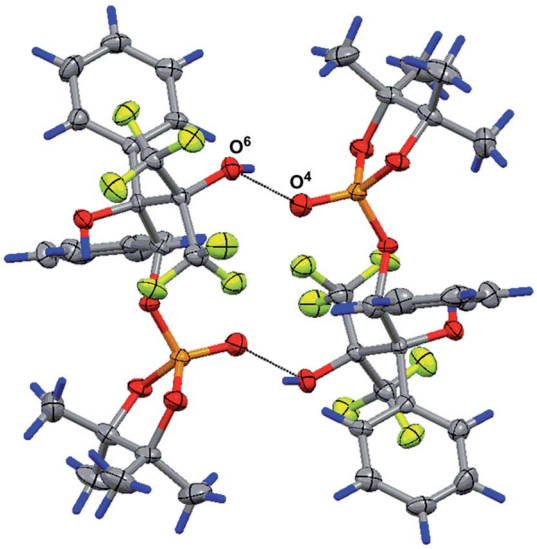

Fig. 8 The system of classical hydrogen bonds in the crystal of **16**.

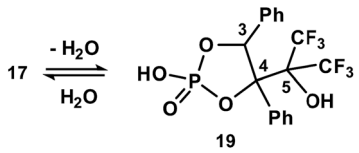

Scheme 5 The equilibrium of phosphates **17** and **19** in dioxane solution.

confirmed by XRD. The geometry of the complex in a crystal and atom numbering are shown in Fig. 9, and the main geometrical parameters (bond lengths and bond and torsion angles) are listed in the figure caption. The phosphorus atom has a distorted tetrahedral configuration, and the configuration of the chiral atoms is $C_S{}^3C_R{}^4/C_R{}^3C_S{}^4$. The conformations of the monophosphate **17** and pinacol molecules along the C^4–C^3, C^5–C^4 and C^6–C^{6a} bonds are shown in Fig. 10. All of them are closely related to the almost regular staggered species. The phenyl substituents are located in the *gauche*-conformation along the C^4–C^3 bond [the torsion angle of C^{13}–C^3–C^4–C^{19} is −50.1(6)°].

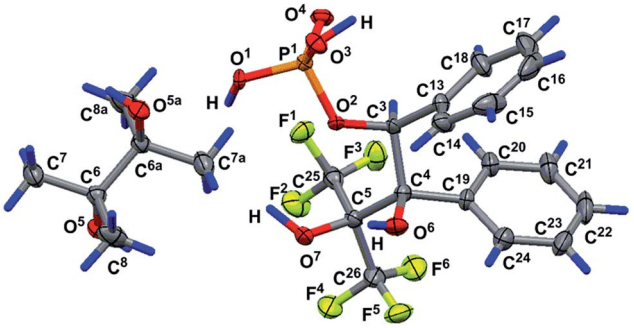

Fig. 9 Geometry of complex **18** in a crystal (solvate of molecule **17** with 1/2 pinacol, racemate, and $C_S{}^3C_R{}^4$-enantiomer is shown). Selected bond lengths (Å) and bond and torsion angles (°): P^1–O^1 1.535(5), P^1–O^2 1.588(4), P^1–O^3 1.551(4), P^1–O^4 1.489(4), O^1–P^1–O^2 103.4(2), O^1–P^1–O^3 102.6(3), O^1–P^1–O^4 116.9(3), O^2–P^1–O^3 109.1(2), O^2–P^1–O^4 111.3(2), O^2–C^3–C^4–C^5 58.8(6), P^1–O^2–C^3–C^4 −168.4(3) and C^3–C^4–C^5–C^{26} −163.4(5).

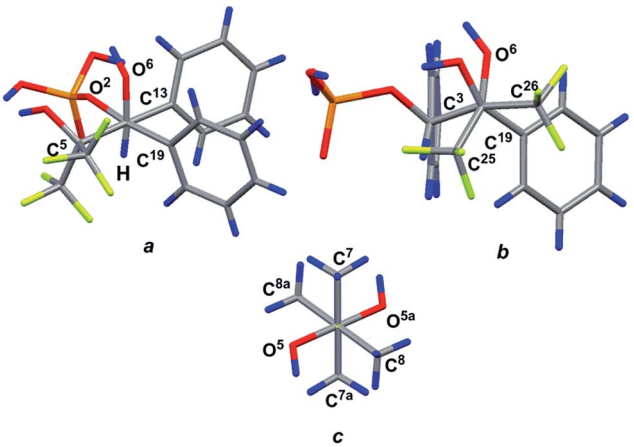

Fig. 10 View of the conformations for the molecule (**17**) in front of the C^4–C^3 (a), C^5–C^4 (b) and C^6–C^{6a} (c) bonds.

The trifluoromethyl groups have different orientations relative to the phenyl ring at the C^4 atom (see Fig. 10) and therefore fluorine atoms exhibit non-equivalence in the ^{19}F NMR spectrum owing to the anisotropy of the phenyl ring.

Due to the classical O–H···O hydrogen bonds of the molecules, **17** and pinacol form sheets along the *b*0*c* crystallographic plane, and thus, a 2D supramolecular structure is realized in the crystal [the parameters of the interactions are O^1–H^1···O(4) interaction: O^1–H^1 0.86(6) Å, H^1···O^4 1.76(6) Å, O^1···O^4 2.547(6) Å, ∠O^1–H^1–O^4 152(9)°, and symmetry operation x, 3/2 − y, 1/2 + z; O^3–H^3···O^5 interaction: O^3–H^3 0.98(7) Å, H^3···O^5 1.68(7) Å, O^3···O^5 2.639(6) Å, ∠O^3–H^3–O^5 165(5)°, and symmetry operation −1 + x, 1 + y, −1 + z; O^7–H^7···O^4 interaction: O^7–H^7 0.99(9) Å, H^7···O^4 1.85(7) Å, O^7···O^4 2.802(6) Å, ∠O^7–H^7–O^4 159(8)°, and symmetry operation x, 3/2 − y, 1/2 + z]. The packing of the molecules **17** in the crystal of solvate **18** is also stabilized by the intramolecular O^7–H^7···F^1 classical hydrogen bond [the parameters are O^7–H^7 0.99(9) Å, H^7···F^1 2.31(9) Å, O^7···F^1 2.757(6) Å, and ∠O^7–H^7–F^1 106(7)°, see ESI†].

Experimental

1-(2,3-Butylenedioxy)-6,6-bis(trifluoromethyl)-3,4-diphenyl-1,2,5,7-phosphatrioxabicyclo[2.2.1^{1,4}]heptane 13

Hexafluoroacetone (4.81 g, 30 mmol) was condensed into a CCl_4/CH_2Cl_2 (1 : 1) solution (40 mL) of dioxaphosphole **12** (10.4 g, 30 mmol) at −40 °C. The reaction mixture was warmed up to 20 °C (10 h) and then evaporated under reduced pressure (14 Torr) to give a white precipitate of **13**, which was filtered off and dried *in vacuo* (14 Torr). Yield 7.12 g (47%), mp 122–125 °C. The filtrate was evaporated *in vacuo* (14 Torr) under an argon atmosphere to give a pale yellow oil, which gradually crystallized under a pentane layer (−18 °C). Clear white crystals of compound **13** were filtered off. Yield 3.62 g (24%), mp 123–125 °C. Anal. calcd for $C_{23}H_{23}F_6O_5P$ (524.12): C, 52.68; H, 4.42; P, 5.91. Found: C, 52.63; H, 4.39; P, 5.98. IR (KBr) (ν_{max}, cm^{-1}): 2987, 2947, 1454, 1398, 1378, 1342, 1277, 1262, 1231, 1199, 1155, 1141, 1080, 1048, 1006, 979, 936, 883, 84, 816, 793, 770, 748, 719, 694, 666, 635, 539, 476. ^1H NMR (400 MHz, $CDCl_3$)/δ (ppm): 7.30 (m, 2H), 7.18 (m, 5H), 7.10 (m, 3H), 5.46 (d, 1H, $^3J_{POCH}$ = 17.0 Hz, H^3), 1.49 (br. s, 12H, CH_3). $^{13}C/^{13}C$–{^1H} NMR (100.6 MHz, $CDCl_3$), (hereinafter a view of signal in ^{13}C–{^1H} NMR spectrum is in parentheses)/δ_C (ppm): 135.74 (m (d), $^3J_{HCCC}$ = 7.7 Hz, $^2J_{HCC}$ = 5.2 Hz, $^3J_{POCC}$ = 0.7 Hz, C^{13}), 133.36 (dt (d), $^3J_{POCC}$ = 12.2 Hz, $^3J_{HCCC}$ = 7.5 Hz, C^{19}), 129.18 (dt (s), $^1J_{HC}$ = 160.7 Hz, $^3J_{HCCC}$ = 7.4 Hz, C^{22}), 128.61 (dm (s), $^1J_{HC}$ = 161.0 Hz, $^3J_{HCCC}$ = 7.2 Hz, C^{16}), 128.09 (br. dd (s), $^1J_{HC}$ = 160.3 Hz, $^3J_{HCCC}$ = 7.4 Hz, $C^{15,17}$), 127.90 (dd (s), $^1J_{HC}$ = 161.0 Hz, $^3J_{HCCC}$ = 7.0 Hz, $C^{21,23}$), 127.21 (br. ddd (s), $^1J_{HC}$ = 159.6 Hz, $^3J_{HCCC}$ = 6.2–6.3 Hz, $^3J_{HCCC}$ = 6.2–6.3 Hz, $C^{14,18}$), 125.82 (ddd (s), $^1J_{HC}$ = 161.1 Hz, $^3J_{HCCC}$ = 7.4 Hz, $^3J_{HCCC}$ = 6.2 Hz, $C^{20,24}$), 122.60 (qd (qd), $^1J_{FC}$ = 285.8 Hz, $^2J_{PCC}$ = 1.1 Hz, C^{26}), 121.71 (br. qd (qd), $^1J_{FC}$ = 289.8 Hz, $^2J_{PCC}$ = 5.7 Hz, C^{25}), 99.76 (ddm (d), $^2J_{POC}$ = 23.9 Hz, $^2J_{HCC}$ = 4.2–4.4 Hz, $^3J_{HCCC}$ = 4.2–4.4 Hz, C^4), 87.68 (dmd (d), $^1J_{HC}$ = 156.3 Hz, $^2J_{POC}$ = 2.9 Hz, $^3J_{HCCC}$ = 4.4 Hz, C^3), 82.93 (m (d), $^2J_{POC}$ = 2.2 Hz, $^2J_{HCC}$ = 4.2–4.4 Hz, $C_{eq.}{}^8$), 79.17 (m (d), $^2J_{POC}$ = 2.9 Hz, $^2J_{HCC}$ = 4.4 Hz, $C_{ax}{}^7$), 77.78 (d. sept (d. sept), $^1J_{PC}$ = 154.8 Hz,

$^{2}J_{FCC}$ = 30.7 Hz, C^{6}), 23.52 (br. qdq (br. d), $^{1}J_{HC}$ = 127.3 Hz, $^{3}J_{POCC}$ = 11.0 Hz, $^{3}J_{HCCC}$ = 4.0 Hz, C^{9-12}). ^{19}F NMR (376.5 MHz, $CDCl_3$)/δ_F (ppm): −68.44 (q. d, $^{4}J_{FCCCF}$ = 10.3 Hz, $^{3}J_{PCCF}$ = 4.6 Hz), −68.87 (q, $^{4}J_{FCCCF}$ = 10.3 Hz, $^{3}J_{PCCF}$ = 2.3 Hz). ^{31}P–{^{1}H}/^{31}P NMR (161.9 MHz, $CDCl_3$)/δ_P (ppm): −25.1 (dd (s), $^{3}J_{PCCH}$ = 17.6 Hz, $^{3}J_{PCCF}$ = 1.9 Hz). ESI-MS (*m*/*z*): 523.97.

1-(2,3-Butylenedioxy)-5,5-bis(trifluoromethyl)-3,4-diphenyl-1,2,6,7-phosphatrioxabicyclo[2.2.1^{1,4}]heptane 14

A mixture of compound **13** (6.00 g, 11.45 mmol) and CH_2Cl_2 (20 mL) was kept for five days (control by ^{31}P NMR). After completion of the rearrangement, the reaction mixture was evaporated *in vacuo* (14 Torr) under an argon atmosphere to give a yellow oily residue, which was gradually crystallized during storage under a pentane layer (−18 °C). The crystalline precipitate of **14** was filtered off and dried *in vacuo* (14 Torr). Yield 5.34 g (89%), mp 125–127 °C. Anal. calcd for $C_{23}H_{23}F_6O_5P$ (524.12): C, 52.68; H, 4.42; P, 5.91. Found: C, 52.64; H, 4.40; P, 5.93. IR (KBr) (ν_{max}, cm^{-1}): 3067, 3036, 2984, 2938, 1500, 1460, 1452, 1396, 1378, 1288, 1241, 1164, 1103, 1042, 1014, 982, 949, 899, 879, 853, 833, 805, 783, 754, 738, 714, 713, 695, 666, 604, 581, 560, 498, 486, 461. ^{1}H NMR (400 MHz, $CDCl_3$)/δ (ppm): 7.44 (m, 1H), 7.30 (m, 1H), 7.17 (m, 3H), 7.08 (m, 5H), 5.72 (d, 1H, $^{3}J_{POCH}$ = 19.2 Hz, H^{3}), 1.52 (s, 3H, CH_3), 1.51 (s, 3H, CH_3), 1.43 (s, 3H, CH_3), 1.38 (s, 3H, CH_3). ^{13}C/^{13}C–{^{1}H} NMR (100.6 MHz, $CDCl_3$)/δ_C (ppm): 135.40 (tt (s), $^{3}J_{HCCC}$ = 5.1–5.3 Hz, $^{2}J_{HCC}$ = 2.2 Hz, C^{13}), 131.08 (dt (d), $^{3}J_{POCC}$ = 18.7 Hz, $^{3}J_{HCCC}$ = 7.2 Hz, C^{19}), 128.59 (dm (s), $^{1}J_{HC}$ = 160.7 Hz, $^{3}J_{HCCC}$ = 7.3 Hz, $^{3}J_{HCCC}$ = 7.3 Hz, C^{16} or C^{22}), 128.56 (dm (s), $^{1}J_{HC}$ = 160.7 Hz, $^{3}J_{HCCC}$ = 7.3 Hz, $^{3}J_{HCCC}$ = 7.3 Hz, C^{16} or C^{22}), 128.52 (dm (s), $^{1}J_{HC}$ = 161.4 Hz, $^{3}J_{HCCC}$ = 7.3 Hz, $^{3}J_{HCCC}$ = 7.3 Hz, $C^{14,18}$), 127.98 (br. dd (s), $^{1}J_{HC}$ = 160.5 Hz, $^{3}J_{HCCC}$ = 7.2 Hz, C^{23}), 127.93 (br. dm (br. sept), $^{1}J_{HC}$ = 160.5 Hz, $^{5}J_{FCCCCC}$ = 1.9 Hz, C^{24}), 127.76 (dm (s), $^{1}J_{HC}$ = 160.7 Hz, $^{3}J_{HCCC}$ = 6.0–7.0 Hz, $C^{15,17}$), 127.13 (br. dd (s), $^{1}J_{HC}$ = 161.4 Hz, $^{3}J_{HCCC}$ = 7.3 Hz, C^{21}), 126.90 br. dm (br. q), $^{1}J_{HC}$ = 160.5 Hz, $^{5}J_{FCCCCC}$ = 5.0 Hz, C^{20}), 122.40 (qd (qd), $^{1}J_{FC}$ = 286.4 Hz, $^{3}J_{POCC}$ = 8.6 Hz, CF_3), 121.08 (qd (qd), $^{1}J_{FC}$ = 289.4 Hz, $^{3}J_{POCC}$ = 2.7 Hz, CF_3), 83.41 (sept (sept), $^{2}J_{CCF}$ = 29.3 Hz, C^{5}), 82.93 (m (d), $^{2}J_{POC}$ = 2.2 Hz, $^{2}J_{HCC}$ = 3.6 Hz, $^{3}J_{HCCC}$ = 3.8 Hz, $C_{eq.}^{7}$), 82.47 (dm (dq), $^{1}J_{HC}$ = 154.8 Hz, $^{2}J_{POC}$ = 2.9 Hz, $^{4}J_{FCCCC}$ = 2.6–2.8 Hz, C^{3}), 79.74 (dt (d), $^{2}J_{POC}$ = 20.2 Hz, $^{3}J_{HCCC}$ = 3.7 Hz, C^{4}), 79.30 (m (d), $^{2}J_{POC}$ = 2.9 Hz, $^{2}J_{HCC}$ = 3.7 Hz, $^{3}J_{HCCC}$ = 3.6–3.7 Hz, C_{ax}^{8}), 23.72 (qdq (d), $^{1}J_{HC}$ = 127.6 Hz, $^{3}J_{POCC}$ = 6.2 Hz, $^{3}J_{HCCC}$ = 4.4 Hz, C^{9}–$C_{eq.}^{7}$), 23.69 (qdq (d), $^{1}J_{HC}$ = 127.6 Hz, $^{3}J_{POCC}$ = 5.2 Hz, $^{3}J_{HCCC}$ = 4.4 Hz, C^{10}–$C_{eq.}^{7}$), 23.54 (qdq (d), $^{1}J_{HC}$ = 127.5 Hz, $^{3}J_{POCC}$ = 7.7 Hz, $^{3}J_{HCCC}$ = 4.4 Hz, C^{11}–C_{ax}^{8}), 23.36 (qdq (d), $^{1}J_{HC}$ = 127.5 Hz, $^{3}J_{POCC}$ = 8.0 Hz, $^{3}J_{HCCC}$ = 4.4 Hz, C^{12}–C_{ax}^{8}). ^{19}F NMR (376.5 MHz, $CDCl_3$)/δ_F (ppm): −68.22 (q, $^{4}J_{FCCCF}$ = 9.5 Hz), −72.35 (q, $^{4}J_{FCCCF}$ = 9.5 Hz). ^{31}P–{^{1}H}/^{31}P NMR (161.9 MHz, $CDCl_3$)/δ_P (ppm): −27.3 (d (s), $^{3}J_{POCH}$ = 20.4 Hz). ESI-MS (*m*/*z*): 523.97.

Hydrolysis of compound 13

To a suspension of compound **13** (1 g, 1.91 mmol) in diethyl ester (5 mL), a solution of 0.1 mL (5.72 mmol) of water in 3 mL of diethyl ester was added dropwise with constant stirring. The resulting white crystalline precipitate of compound **15** (hydrate with one H_2O molecule) was filtered off and dried *in vacuo* (14 Torr). Yield 0.31 g (83%), mp 190–192 °C. ^{1}H NMR (400 MHz, DMF-d_7), δ: 8.72 (br. s, 1H, OH), 1.41 (br. s, 12H, H^{9-12}). ^{31}P–{^{1}H} NMR (161.9 MHz, DMF-d_7), δ_P: 10.6 ppm (s). The ^{1}H NMR spectral data of an aliquot of the filtrate contain the benzoin and hexafluoroisopropanol signals. The structure of hexafluoroisopropanol was proven by a comparison of its spectral characteristics (^{1}H, ^{13}C, ^{19}F NMR) with previously published data.[43] The filtrate was evaporated *in vacuo* (14 Torr) to give a white precipitate of benzoin, mp 132–134 °C. ^{1}H NMR (600.0 MHz, acetone-d_6/$CDCl_3$ = 2 : 1)/δ (ppm): 8.03 (m, 2H, *XX*′-part of *AA*′*XX*′-subsystem, $^{3}J_{AX} = {}^{3}J_{A'X'}$ = 7.5 Hz, $H^{20,24}$), 7.56 (tt, 1H, $^{3}J_{AM} = {}^{3}J_{A'M}$ = 7.5 Hz, $^{4}J_{XM} = {}^{4}J_{X'M'}$ = 1.5 Hz, *M*-part of *AA*′*MXX*′-system, H^{22}), 7.45 (br. dd, 2H, *AA*′-part of *AA*′*XX*′-subsystem, $^{3}J_{AX} = {}^{3}J_{A'X'}$ = 7.5 Hz, $^{3}J_{AM} = {}^{3}J_{A'M'}$ = 7.5 Hz, $H^{21,23}$), 7.44 (m, 2H, *XX*′-part of *AMM*′*XX*′-system, $^{3}J_{XM} = {}^{3}J_{X'M'}$ = 7.5 Hz, $H^{14,18}$), 7.32 (br dd, 2H, *MM*′-part of *AMM*′*XX*′-system, $^{3}J_{XM} = {}^{3}J_{X'M'}$ = 7.5 Hz, $^{3}J_{AM} = {}^{3}J_{AM'}$ = 7.5 Hz, $H^{15,17}$), 7.25 (tt, 1H, *A*-part of *AMM*′*XX*′-system, $^{3}J_{AM} = {}^{3}J_{AM'}$ = 7.5 Hz, $^{4}J_{AX} = {}^{4}J_{AX'}$ = 1.5 Hz, H^{16}), 6.13 (s, 1H, H^{3}), 4.93 (br. s, 1H, OH). ^{13}C/^{13}C–{^{1}H} NMR (150.0 MHz, acetone-d_6/$CDCl_3$ = 2 : 1)/δ_C (ppm): 200.01 (br. dt (s), $^{2}J_{HC^3C^4}$ = 3.5 Hz, $^{3}J_{HC^{20,24}CC^4}$ = 3.3 Hz, C^{4}), 140.75 (tdd (s), $^{3}J_{HC^{15,17}CC^{13}}$ = 7.5 Hz, $^{2}J_{HC^3C^{13}}$ = 5.5 Hz, $^{3}J_{HOCC^{13}}$ = 1.3 Hz, C^{13}), 135.36 (br. t (s), $^{3}J_{HC^{21,23}CC^{19}}$ = 7.4 Hz, C^{19}), 134.27 (dt (s), $^{1}J_{HC^{22}}$ = 162.9 Hz, $^{3}J_{HC^{20,24}CC^{22}}$ = 7.7 Hz, C^{22}), 129.86 (ddddd (s), $^{1}J_{HC^{20,24}}$ = 161.3 Hz, $^{3}J_{HC^{24,20}CC^{20,24}}$ = 7.6 Hz, $^{3}J_{HC^{22}CC^{20,24}}$ = 7.6 Hz, $^{2}J_{HC^{21,23}C^{20,24}}$ = 1.7 Hz, $^{4}J_{HC^4CCC^{20,24}}$ = 1.3 Hz, $C^{20,24}$), 129.52 (br. dm (s), $^{1}J_{HC^{15,17}}$ = 161.5–161.8 Hz, $^{3}J_{HC^{15,17}CC^{17,15}}$ = 6.0–7.0 Hz, $C^{15,17}$), 129.41 (dd (s), $^{1}J_{HC^{21,23}}$ = 161.7 Hz, $^{3}J_{HC^{23,21}CC^{21,23}}$ = 7.6 Hz, $C^{21,23}$), 128.84 (dtd (s), $^{1}J_{HC^{16}}$ = 161.0 Hz, $^{3}J_{HC^{14,18}CC^{16}}$ = 7.6 Hz, $^{5}J_{HC^3CCCC^{16}}$ = 1.1 Hz, C^{16}), 128.44 (dm (s), $^{1}J_{HC^{14,18}}$ = 162.4 Hz, $^{3}J_{HC^{18,14}CC^{14,18}}$ = 6.5–7.5 Hz, $^{3}J_{HC^{16}CC^{14,18}}$ = 6.5–7.5 Hz, $^{3}J_{HC^3CC^{14,18}}$ = 4.5 Hz, $C^{14,18}$), 76.94 (dt (s), $^{1}J_{HC^3}$ = 146.8 Hz, $^{3}J_{HC^{14,18}CC^3}$ = 4.0 Hz, C^{3}). ^{13}C–{^{1}H} NMR (100.6 MHz, $CDCl_3$), δ_C: 199.15 (br. dt (s), $^{2}J_{HC^3C^4}$ = 3.3 Hz, $^{3}J_{HC^{20,24}CC^4}$ = 3.3 Hz, C^{4}), 139.20 (tdd (s), $^{3}J_{HC^{15,17}CC^{13}}$ = 7.3 Hz, $^{2}J_{HC^3C^{13}}$ = 5.5 Hz, $^{3}J_{HOCC^{13}}$ = 2.2 Hz, C^{13}), 133.74 (br. t (s), $^{3}J_{HC^{21,23}CC^{19}}$ = 7.7 Hz, C^{19}), 134.07 (br. td (s), $^{1}J_{HC^{22}}$ = 162.2 Hz, $^{3}J_{HC^{20,24}CC^{22}}$ = 7.7 Hz, C^{22}), 129.33 (ddddd (s), $^{1}J_{HC^{20,24}}$ = 160.7 Hz, $^{3}J_{HC^{24,20}CC^{20,24}}$ = 7.6 Hz, $^{3}J_{HC^{22}CC^{20,24}}$ = 7.6 Hz, $^{2}J_{HC^{21,23}C^{20,24}}$ = 1.4 Hz, $^{4}J_{HC^4CCC^{20,24}}$ = 1.2 Hz, $C^{20,24}$), 129.30 (br. dd (s), $^{1}J_{HC^{15,17}}$ = 161.0 Hz, $^{3}J_{HC^{15,17}CC^{17,15}}$ = 6.5–7.0 Hz, $C^{15,17}$), 128.86 (dd (s), $^{1}J_{HC^{21,23}}$ = 162.5 Hz, $^{3}J_{HC^{23,21}CC^{21,23}}$ = 7.7 Hz, $C^{21,23}$), 128.76 (dtt (s), $^{1}J_{HC^{16}}$ = 161.0 Hz, $^{3}J_{HC^{14,18}CC^{16}}$ = 7.2 Hz, $^{2}J_{HC^{15,17}C^{16}}$ = 1.5 Hz, C^{16}), 127.96 (dm (s), $^{1}J_{HC^{14,18}}$ = 162.4 Hz, $^{3}J_{HC^{18,14}CC^{14,18}}$ = 6.5–7.5 Hz, $^{3}J_{HC^{16}CC^{14,18}}$ = 6.5–7.5 Hz, $^{3}J_{HC^3CC^{14,18}}$ = 4.5 Hz, $C^{14,18}$), 76.42 (dtd (s), $^{1}J_{HC^3}$ = 146.8 Hz, $^{3}J_{HC^{14,18}CC^3}$ = 3.4 Hz, $^{2}J_{HOC^3}$ = 1.5 Hz, C^{3}).

Hydrolysis of compound 14

To a suspension of compound **14** (3.54 g, 6.75 mmol) in 10 mL of diethyl ester, a solution of 0.12 mL (6.75 mmol) of water in 5 mL of diethyl ester was added dropwise with constant stirring. The resulting white crystalline precipitate of compound **16** was filtered off and dried *in vacuo* (14 Torr). Yield 3.01 g (82%), mp 155–156 °C. Anal. calcd for $C_{23}H_{25}F_6O_6P$ (542.41): C, 50.93; H, 4.65; P, 5.71. Found: C, 50.94; H, 4.60; P, 5.73. IR (nujol) (ν_{max}, cm^{-1}): 3606, 3214, 2993, 1498, 1451, 1397, 1385, 1262, 1225,

1206, 1145, 1134, 1006, 993, 962, 930, 910, 815, 806, 724, 713, 700, 616, 594, 549, 497, 414. ^{1}H NMR (400 MHz, DMF-d_7)/δ (ppm): 8.74 (br. s, 1H, OH), 7.60 (d, 2H, $^{3}J_{HCCH}$ 5.6 Hz, $H^{20,24}$), 7.23 (m, 2H, $^{3}J_{HCCH}$ = 6.7–7.7 Hz, $^{5}J_{PCCCCH}$ = 1.5 Hz, $H^{14,18}$), 7.11 (m, 3H, H^{21-23}), 7.05 (m, 3H, H^{15-17}), 6.25 (d, 1H, $^{3}J_{POCH}$ = 7.6 Hz, H^{3}), 5.98 (s, 1H, OH), 1.49 (s, 3H, Me), 1.42 (s, 6H, Me), 1.26 (s, 3H, Me). ^{13}C/^{13}C–{^{1}H} NMR (100.6 MHz, DMF-d_7)/δ_C (ppm): 139.45 (br. td (br. s), $^{3}J_{HCCC}$ = 6.2, $^{2}J_{HCC}$ = 5.2, C^{13}), 138.09 (ddd (s), $^{3}J_{HCCC}$ = 7.2 Hz, $^{3}J_{HCCC}$ = 6.7 Hz, $^{3}J_{HCCC}$ = 3.7 Hz, C^{19}), 130.91 (dddd (s), $^{1}J_{HC}$ = 163.3 Hz, $^{3}J_{HCCC}$ = 5.4 Hz, $^{3}J_{HCCC}$ = 5.2 Hz, $^{3}J_{HCCC}$ = 5.2 Hz, $C^{14,18}$), ~129.2 (v. br. d (v. br. s) C^{20}), 128.53 (dt (s), $^{1}J_{HC}$ = 160.0 Hz, $^{3}J_{HCCC}$ = 7.4 Hz, C^{16}), 128.13 (dt (s), $^{1}J_{HC}$ = 160.0 Hz, $^{3}J_{HCCC}$ = 7.7 Hz, C^{22}), 127.69 (br. dd (s), $^{1}J_{HC}$ = 161.8 Hz, $^{3}J_{HCCC}$ = 5.0–6.0 Hz, $C^{15,17}$), 127.37 (v. br. d (v. br. s), $^{1}J_{HC}$ ~160.0–162.0 Hz, $C^{21,23,24}$), 124.80 (q (q), $^{1}J_{FC}$ = 291.6 Hz, CF_3), 124.58 (q (q), $^{1}J_{FC}$ = 291.1 Hz, CF_3), 89.33 (m (d), $^{2}J_{POC}$ = 1.2 Hz, C^{7} or C^{8}), 89.23 (m (s), C^{8} or C^{7}), 83.34 (sept (sept), $^{2}J_{FCC}$ = 25.6 Hz, C^{5}), 82.89 (br. dm (br. d), $^{1}J_{HC}$ = 149.5 Hz, $^{2}J_{POC}$ = 5.1 Hz, C^{3}), 81.75 (br. d (d), $^{3}J_{POCC}$ = 10.0 Hz, C^{4}), 24.76, 24.27, 24.14 and 23.97 ppm (four qdq (four d), $^{1}J_{HC}$ = 127.5, 127.5, 127.8 and 127.9 Hz, $^{3}J_{POCC}$ = 4.4, 7.0, 3.9 and 6.5 Hz, $^{3}J_{HCCC}$ = 4.3–4.4 Hz, C^{9-12}). ^{19}F NMR (376.4 MHz, DMF-d_7)/δ_F (ppm): −67.43 (q, $^{4}J_{FCCCF}$ = 11.3 Hz), −68.19 (q, $^{4}J_{FCCCF}$ = 11.3 Hz). ^{31}P/^{31}P–{^{1}H} NMR (161.9 MHz, DMF-d_7)/δ_P (ppm): 11.0 (d (s), $^{3}J_{PCCH}$ = 5.9 Hz). ^{13}C/^{13}C–{^{1}H} NMR (100.6 MHz, DMSO-d_6)/δ_C (ppm): 139.45 (br. td (br. s), C^{13}), 137.0 (m (s), C^{19}), 129.63 (dddd (s), $^{1}J_{HCCC}$ = 160.0 Hz, $^{3}J_{HCCC}$ = 6.0–7.0 Hz, $^{3}J_{HCCC}$ = 6.0–7.0 Hz, $^{3}J_{HCCC}$ = 4.4 Hz, $C^{14,18}$), ~129.2 (v. br. d (v. br. s) C^{20}), 127.65 (dt (s), $^{1}J_{HC}$ = 160.0 Hz, $^{3}J_{HCCC}$ = 7.3 Hz, C^{16}), 127.28 (dt (s), $^{1}J_{HC}$ = 160.0 Hz, $^{3}J_{HCCC}$ = 7.7 Hz, C^{22}), 126.81 (dd (s), $^{1}J_{HC}$ = 160.0 Hz, $^{3}J_{HCCC}$ = 6.6 Hz, $C^{15,17}$), ~126.9 (v. br. d (v. br. s), $^{1}J_{HC}$ ~160.0–162.0 Hz, $C^{21,23,24}$), 124.68 (q (q), $^{1}J_{FC}$ = 292.0 Hz, CF_3), 123.45 (q (q), $^{1}J_{FC}$ = 290.5 Hz, CF_3), 89.31 (m (s), C^{7} or C^{8}), 88.18 (m (s), C^{8} or C^{7}), 82.01 (sept (sept), $^{2}J_{FCC}$ = 25.6 Hz, C^{5}), 81.29 (br. dm (br. d), $^{1}J_{HC}$ = 149.0 Hz, $^{2}J_{POC}$ = 4.8 Hz, C^{3}), 80.59 (br. d (d), $^{3}J_{POCC}$ = 9.9 Hz, C^{4}), 24.24, 23.72, 23.55 and 23.37 (four qdq (four d), $^{1}J_{HC}$ = 127.6, 127.6, 128.4 and 129.1 Hz, $^{3}J_{POCC}$ = 3.7, 7.0, 3.3 and 6.2 Hz, $^{3}J_{HCCC}$ = 3.0–3.3 Hz, C^{9-12}). ^{19}F NMR (376.4 MHz, DMSO-d_6)/δ_F (ppm): −66.49 (br. q, $^{4}J_{FCCCF}$ = 10.9 Hz), −68.10 (br. q, $^{4}J_{FCCCF}$ = 10.9 Hz). ^{31}P/^{31}P–{^{1}H} NMR (161.9 MHz, DMSO-d_6)/δ_P (ppm): 10.7 (d (s), $^{3}J_{PCCH}$ = 7.8 Hz). MALDI-MS (m/z): 565.03 (M + Na), 580.93 (M + K).

Hydrolysis of compound 16

Compound **16** (1.50 g, 2.77 mmol) was refluxed in a solution (15 mL) of dioxane and H_2O (2 : 1) for 20 hours (control by ^{31}P NMR). ^{31}P/^{31}P–{^{1}H} NMR (161.9 MHz, dioxane/δ_P (ppm): −1.2 (d (s), $^{3}J_{PCCH}$ = 5.6 Hz), 14.0 (br. s (s)). ^{19}F NMR (376.4 MHz, $CDCl_3$)/δ_F (ppm): −67.39 (q, $^{4}J_{FCCCF}$ = 10.9 Hz), −68.65 (q, $^{4}J_{FCCCF}$ = 10.9 Hz), −68.65 (q, $^{4}J_{FCCCF}$ = 10.9 Hz), −69.98 (q, $^{4}J_{FCCCF}$ = 9.5 Hz). After completion of the hydrolysis, the reaction mixture was evaporated *in vacuo* (14 Torr) to give a yellow oily residue, which was crystallized from CH_2Cl_2 (10 mL). The crystalline precipitate of **18** (adduct with pinacol) was filtered off and dried *in vacuo* (14 Torr). Yield 1.01 g (63%), mp 99–103 °C. Anal. calcd for $C_{23}H_{29}F_6O_8P$ (578.44): C, 47.76; H, 5.05; P, 5.35. Found: C, 47.74; H, 5.00; P, 5.31. IR (nujol) (ν_{max}, cm^{-1}): 3524, 3499, 3282, 3068, 2349, 1736, 1681, 1601, 1497, 1452, 1377, 1277, 1213, 1154, 1111, 1074, 1022, 1001, 967, 935, 761, 727, 711, 699, 624, 612, 541, 523, 494, 463. ^{1}H NMR (400 MHz, CD_3CN)/δ (ppm): 7.46 (br. d, 2H, $H^{20,24}$), 7.21 (d, $^{3}J_{HCCH}$ = 7.1 Hz, 2H, $H^{14,18}$), 7.10 (m, 3H, $H^{19,20,21}$), 7.04 (m, 3H, $H^{15,16,17}$), 6.09 (d, $^{3}J_{POCH}$ = 4.9 Hz, 1H, H^{3}), 1.16 (s, 12H, Me, pinacol). ^{13}C/^{13}C–{^{1}H} NMR (100.6 MHz, CD_3CN)/δ_C (ppm): 137.98 (br. td (s), $^{2}J_{HCC}$ = 5.5, C^{19}), 137.07 (br. td (br. s), $^{3}J_{HCCC}$ 7.3 Hz, C^{13}), 131.10 (br. d (s), $^{1}J_{HCCC}$ = 156.6 Hz, $C^{14,18}$), ~127.9 (v. br. d (v. br. s) $C^{20,24}$), 128.71 (br. dt (s), $^{1}J_{HC}$ 161.4 Hz, C^{16}), 128.64 (br. dt (s), $^{1}J_{HC}$ 161.7 Hz, C^{22}), 128.10 (br. dd (s), $^{1}J_{HC}$ = 158.5 Hz, $^{3}J_{HCCC}$ = 7.3 Hz, $C^{15,17}$), 127.85 and 126.74 (two v. br. d (two v. br. s), $C^{20,24}$ and $C^{21,23}$), 124.35 (q (q), $^{1}J_{FC}$ = 289.4 Hz, CF_3), 124.18 (q (q), $^{1}J_{FC}$ = 290.9 Hz, CF_3), 90.34 (m (s), pinacol), 83.79 (sept (sept), $^{2}J_{FCC}$ = 25.7 Hz, C^{5}), 83.12 (d. m (d), $^{1}J_{HC}$ = 151.5 Hz, $^{2}J_{POC}$ = 2.6 Hz, C^{3}), 81.87 (m (d), $^{3}J_{POCC}$ = 8.1 Hz, C^{4}), 25.16 (q (s), $^{1}J_{HC}$ = 125.4, CH_3, pinacol). ^{19}F NMR (376.4 MHz, $CDCl_3$/DMSO-d_6 (3 : 1))/δ_F (ppm): −67.05 (q, $^{4}J_{FCCCF}$ = 11.2 Hz), −67.82 (q, $^{4}J_{FCCCF}$ = 10.2 Hz). ^{31}P/^{31}P–{^{1}H}NMR (161.9 MHz, CD_3CN)/δ_P (ppm): −1.4 (br. s (s)).

Crystal structure determination

Crystal structures were determined by X-ray diffraction of suitable monocrystals. Crystal data were collected at 296 K using graphite monochromatic MoK_α (0.71073 Å) radiation and ω-scan. Data collection images were indexed, integrated, and scaled using the APEX2 data reduction package.[46] Multi-scan empirical absorption corrections were applied to all data sets, where appropriate, using the SADABS program.[47] The structures were solved and refined using the SHELX[48] program. All crystal structure pictures were created using Mercury CSD 2.4.[49]

Crystal data for 13

$C_{23}H_{23}F_6O_5P$, M = 524.38, monoclinic, a = 9.485(6), b = 11.002(7), c = 12.115(8) Å, β = 101.517(8)°, V = 1239(1) Å^3, T = 296 K, space group $P2_1$ (no. 4), Z = 2, 12 827 reflections measured, 4529 unique (R^{int} = 0.071), which were used in all calculations. Final indices R_1 = 0.0667, wR_2 = 0.1629 for 2921 reflections with $I > 2\sigma(I)$; R_1 = 0.1100, wR_2 = 0.2021 for all data.

Crystal data for 14

$C_{23}H_{23}F_6O_5P$, M = 524.38, orthorhombic, a = 12.650(5), b = 16.695(6), c = 22.988(9) Å, V = 4855(3) Å^3, T = 296 K, space group $Pbca$ (no. 61), Z = 8, 28 292 reflections measured, 4766 unique (R^{int} = 0.066), which were used in all calculations. Final indices R_1 = 0.0520, wR_2 = 0.1426 for 2856 reflections with $I > 2\sigma(I)$; R_1 = 0.0985, wR_2 = 0.1825 for all data.

Crystal data for 15

$C_6H_{15}O_5P$, M = 198.15, orthorhombic, a = 6.39(2), b = 10.62(3), c = 14.67(3) Å, V = 995(4) Å^3, T = 296 K, space group $P2_12_12_1$ (no. 19), Z = 4, 5025 reflections measured, 1949 unique (R^{int} = 0.068), which were used in all calculations. Final indices R_1 =

0.0499, wR_2 = 0.1437 for 1316 reflections with $I > 2\sigma(I)$; R_1 = 0.0907, wR_2 = 0.1841 for all data.

Crystal data for 16

$C_{23}H_{25}F_6O_6P$, M = 542.40, triclinic, a = 10.788(13), b = 10.889(13), c = 12.329(15) Å, α = 70.63(2), β = 71.74(2), γ = 67.88(2)°, V = 1236(3) Å^3, T = 296 K, space group $P\bar{1}$ (no. 2), Z = 2, 4706 reflections measured, which were used in all calculations. Final indices R_1 = 0.0880, wR_2 = 0.2734 for 2147 reflections with $I > 2\sigma(I)$; R_1 = 0.1946, wR_2 = 0.3522 for all data.

Crystal data for 18

$C_{17}H_{15}F_6O_6P$ $0.5C_6H_{14}O_2$, M = 519.34, monoclinic, a = 18.721(8), b = 13.944(6), c = 8.706(4) Å, β = 95.489(8)°, V = 2262(2) Å^3, T = 296 K, space group $P2_1/c$ (no. 14), Z = 4, 11 470 reflections measured, 4448 unique (R^{int} = 0.152), which were used in all calculations. Final indices R_1 = 0.0773, wR_2 = 0.1632 for 1683 reflections with $I > 2\sigma(I)$; R_1 = 0.2229, wR_2 = 0.2372 for all data.

Conclusions

It was shown that the reaction of 4,4,5,5-tetramethyl-2-(2-oxo-1,2-diphenyl)ethoxy-1,3,2-dioxaphospholane **12** with hexafluoroacetone results in the simultaneous formation of regioisomeric cage (P–C/P–O)-phosphoranes **13** and **14** in the ratio of 10 : 1. In dichloromethane solution (20 °C, 5 days), the rearrangement of P–C-isomer **13** to P–O-isomer **14** proceeds with high stereoselectivity (>96%). The P–C-isomer hydrolysis unexpectedly leads to the formation of 2-hydroxy-4,4,5,5-tetramethyl-2-oxo-1,3,2-dioxaphospholane with high chemoselectivity. Hydrolysis of the P–O-isomer results in the formation of one stereoisomer of 2-(2,3-dihydroxy-1,2-diphenyl-3-trifluoromethyl-4,4,4-trifluorobutyloxy)-4,4,5,5-tetramethyl-2-oxo-1,3,2-dioxaphospholane with the same configurations for the C^3 and C^4 atoms, and further hydrolysis of this compound yields 2,3-dihydroxy-3-trifluoromethyl-4,4,4-trifluoro-1,2-diphenyl butylphosphate **17** and pinacol.

Acknowledgements

Financial support from the Russian Foundation for Basic Research (Grant No. 16-03-00451) is gratefully acknowledged.

Notes and references

1 K. N. Allen and D. Dunaway-Mariano, *Trends Biochem. Sci.*, 2004, **29**, 495.
2 L. W. Tremblay, G. Zhang, J. Dai, D. Dunaway-Mariano and K. N. Allen, *J. Am. Chem. Soc.*, 2005, **127**, 5298.
3 A. C. Hengge, *Adv. Phys. Org. Chem.*, 2005, **40**, 49.
4 J. K. Lassila, J. G. Zalatan and D. Herschlag, *Annu. Rev. Biochem.*, 2011, **80**, 669.
5 N. J. Baxter, M. W. Bowler, T. Alizadeh, M. J. Cliff, A. M. Hounslow, B. Wu, D. B. Berkowitz, N. H. Williams, G. M. Blackburn and J. P. Waltho, *Proc. Natl. Acad. Sci. U. S. A.*, 2010, **107**, 4555.
6 H. Gu, S. Zhang, K.-Y. Wong, B. K. Radak, T. Dissanayake, D. L. Kellerman, Q. Dai, M. Miyagi, V. E. Anderson, D. M. York, J. A. Piccirilli and M. E. Harris, *Proc. Natl. Acad. Sci. U. S. A.*, 2013, **110**, 13002.
7 N. J. DeYonker and C. E. Webster, *Biochemistry*, 2015, **54**, 4236.
8 G. Baccolini, *Phosphorus, Sulfur Silicon Relat. Elem.*, 2015, **190**, 2173.
9 M. A. van Bochove, M. Swart and F. M. Bickelhaupt, *J. Am. Chem. Soc.*, 2006, **128**, 10738.
10 M. A. van Bochove, M. Swart and F. M. Bickelhaupt, *ChemPhysChem*, 2007, **8**, 2452.
11 S. Dey, *Am. J. Org. Chem.*, 2015, **5**, 83.
12 *Best Synthetic Methods: Organophosphorus (V) Chemistry*, ed. C. Timperley, Elsevier, 2015, ISBN: 9780080982120.
13 W. Phakhodee, S. Wangngae and M. Pattarawarapan, *RSC Adv.*, 2016, **6**, 60287.
14 P. A. Byrne and D. G. Gilheany, *Chem. Soc. Rev.*, 2013, **42**, 6670.
15 D. J. Carr, J. J. S. Kudavalli, K. S. Dunne, H. Müller-Bunz and D. G. Gilheany, *J. Org. Chem.*, 2013, **78**, 10500.
16 E. V. Jennings, K. Nikitin, Y. Ortin and D. G. Gilheany, *J. Am. Chem. Soc.*, 2014, **136**, 16217.
17 K. C. Kumara Swamy, N. N. Bhuvan Kumar, E. Balaraman and K. V. P. Pavan Kumar, *Chem. Rev.*, 2009, **109**, 2551.
18 (*a*) S. Fletcher, *Org. Chem. Front.*, 2015, **2**, 739; (*b*) D. Camp, M. von Itzstein and I. D. Jenkins, *Tetrahedron*, 2015, **71**, 4946.
19 S. Wangngae, C. Duangkamol, M. Pattarawarapan and W. Phakhodee, *RSC Adv.*, 2015, **5**, 25789.
20 S. Cao, P. Gao, Y. Guo, H. Zhao, J. Wang, Y. Liu and Y. Zhao, *J. Org. Chem.*, 2013, **78**, 11283.
21 W. Dai, Q. Liu, X. You, Z. Zhou, Y. Guo, Y. Zhao and S. Cao, *Heteroat. Chem.*, 2016, **27**, 63.
22 X. You, L. Qi, J. Zheng, W. Dai, Y. Guo, Y. Zhao and S. Cao, *Heteroat. Chem.*, 2015, **26**, 168.
23 J. Bader, N. Ignat'ev and B. Hoge, *Inorg. Chem.*, 2014, **53**, 7547.
24 S. M. McCarthy, Y.-C. Lin, D. Devarajan, J. W. Chang, H. P. Yennawar, R. M. Rioux, D. H. Ess and A. T. Radosevich, *J. Am. Chem. Soc.*, 2014, **136**, 4640.
25 O. Fliss, A. Mejri, K. Essalah, M.-T. Boisdon and B. Tangour, *C. R. Chim.*, 2016, **19**, 585.
26 N. V. Ignat'ev, J. Bader, K. Koppe, B. Hoge and H. Willner, *J. Fluorine Chem.*, 2015, **171**, 36.
27 R. Pajkert and G.-V. Röschenthaler, Pentacoordinated and hexacoordinated compounds. Ch. 8, *Organophosphorus Chem.*, 2015, 378–396.
28 (*a*) R. R. Holmes, *Pentacoordinated Phosphorus – Structure and Spectroscopy (ACS Monograph 175)*, Am. Chem. Soc., Washington, DC, 1980; (*b*) R. R. Holmes, *Pentacoordinated Phosphorus – Reaction Mechanisms (ACS Monograph 176)*, Am. Chem. Soc., Washington, DC, 1980.
29 D. E. C. Corbridge, *Phosphorus 2000. Chemistry, Biochemistry and Technology*, Elsevier, Amsterdam, Lausanne, New-York, Oxford, Shannon, Singapore, Tokyo, 2000, ISBN: 0444825509.

30 L. M. Abdrakhmanova, V. F. Mironov, T. A. Baronova, M. N. Dimukhametov, D. B. Krivolapov, I. A. Litvinov, A. A. Balandina, S. K. Latypov and A. I. Konovalov, *Mendeleev Commun.*, 2006, **16**, 320.

31 L. M. Abdrakhmanova, V. F. Mironov, T. P. Gryaznova, S. A. Katsyuba and M. N. Dimukhametov, *Phosphorus, Sulfur Silicon Relat. Elem.*, 2011, **186**, 652.

32 V. F. Mironov, M. N. Dimukhametov, E. V. Mironova, D. B. Krivolapov and L. M. Abdrakhmanova, *Russ. J. Gen. Chem.*, 2015, **85**, 441.

33 V. F. Mironov, M. N. Dimukhametov, E. V. Mironova, D. B. Krivolapov, G. A. Ivkova and L. M. Abdrakhmanova, *Russ. J. Gen. Chem.*, 2015, **85**, 450.

34 V. F. Mironov, T. A. Baronova, E. V. Mironova, M. N. Dimukhametov, D. B. Krivolapov and L. M. Abdrakhmanova, *Russ. J. Org. Chem.*, 2015, **51**, 401.

35 A. N. Pudovik, I. V. Konovalova and E. A. Ishmaeva, *Reactions and methods of investigation of organic compounds (In Russ.)*, ed. B. A. Kazansky, I. L. Knunyants, M. M. Shemyakin and N. N. Melnikov, Chemistry Publish., Moscow, 1973, vol. 23, p. 488.

36 K. Pallitsch, A. Roller and F. Hammerschmidt, *Chem.–Eur. J.*, 2015, **21**, 10200.

37 V. F. Mironov, M. N. Dimukhametov, S. V. Efimov, R. M. Aminova, F. K. Karataeva, D. B. Krivolapov, E. V. Mironova and V. V. Klochkov, *J. Org. Chem.*, 2016, **81**, 5837.

38 (*a*) G. V. Romanov, M. S. Yagfarov, A. I. Konovalov, A. N. Pudovik, I. V. Konovalova and T. N. Yusupova, *Zh. Obshch. Khim.*, 1973, **43**, 2378; (*b*) A. N. Pudovik, I. V. Konovalova, N. P. Anoshina and G. V. Romanov, *Zh. Obshch. Khim.*, 1973, **43**, 2153; (*c*) E. N. Ofitserov, V. F. Mironov, T. N. Sinyashina, A. N. Chernov, I. V. Konovalova, A. V. Il'yasov and A. N. Pudovik, *Dokl. Chem.*, 1989, **306**, 146.

39 N. R. Khasiyatullina, V. F. Mironov, E. V. Mironova, D. B. Krivolapov and I. A. Litvinov, *Russ. J. Gen. Chem.*, 2016, **86**, 551.

40 J. Pesch, K. Harms and T. Bach, *Eur. J. Org. Chem.*, 2004, 2025.

41 S. E. Denmark and Y. Fan, *J. Org. Chem.*, 2005, **70**, 9667.

42 M. Baranac-Stojanovic, R. Markovic and M. Stojanovic, *Tetrahedron*, 2011, **67**, 8000.

43 T. Hayasaka, Y. Katsuhara, T. Kume and T. Yamazaki, *Tetrahedron*, 2011, **67**, 2215.

44 J. R. Cox and M. G. Newton, *J. Org. Chem.*, 1969, **34**, 2600.

45 L. Labaudiniere, Y. Leroux and R. Burgada, *J. Org. Chem.*, 1987, **52**, 157.

46 *APEX2 (Version 2.1), SAINTPlus. Data Reduction and Correction Program, Version 7.31A, Bruker Advansed X-ray Solutions*, BrukerAXS Inc., Madison, Wisconsin, USA, 2006.

47 G. M. Sheldrick, *SADABS, Program for empirical X-ray absorption correction*, Bruker-Nonis, 1990.

48 G. M. Sheldrick, *Acta Crystallogr., Sect. A: Found. Crystallogr.*, 2008, **64**, 112.

49 C. F. Macrae, I. J. Bruno, J. A. Chisholm, P. R. Edgington, P. McCabe, E. Pidcock, L. Rodriguez-Monge, R. Taylor, J. van de Streek and P. A. Wood, *J. Appl. Crystallogr.*, 2008, **41**, 466.